Chemosphere 241 (2020) 124982

Contents lists available at ScienceDirect

Chemosphere

journal homepage: www.elsevier.com/locate/chemosphere

Biofiltration of acetaldehyde resulting from ethanol manufacturing facilities

Chris Duerschner [a], Ashraf Aly Hassan [a, b, *], Bruce Dvorak [a]

[a] University of Nebraska Lincoln, United States
[b] United Arab Emirates University, United Arab Emirates

HIGHLIGHTS

- High thermophilic acetaldehyde removal was achieved at low loading rates.
- Thermophilic removal suffered significantly at higher influent concentrations.
- At room temperature, a maximum elimination capacity of 112 g m^{-3} hr^{-1} is achieved.
- The main biodegradation byproduct of acetaldehyde is acetic acid.

GRAPHICAL ABSTRACT

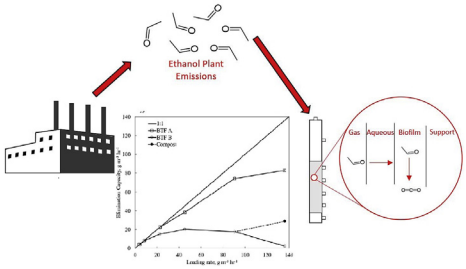

ARTICLE INFO

Article history:
Received 8 August 2019
Received in revised form
24 September 2019
Accepted 26 September 2019
Available online 30 September 2019

Handling Editor: Yongmei Li

Keywords:
Acetaldehyde
Biofiltration
Biotrickling filter (BTF)
HAPs
Thermophilic

ABSTRACT

At ethanol plants, the control of acetaldehyde emissions is accomplished by scrubbers and regenerative thermal oxidizers. However, their operation imposes substantial operating costs. Alternatively, two biotrickling filters were operated in parallel under acetaldehyde loadings ranging from 4 to 136 g m^{-3} hr^{-1}. One filter was operated at room temperature while the other one was heated to 60 °C, to mimic hot drier emissions. The unheated filter maintained 100% removal efficiency up to 45.28 g m^{-3} hr^{-1} loading rate at 30-s empty bed residence time. Highest elimination capacity recorded was 112 g m^{-3} hr^{-1} at 83.2% removal efficiency. The heated filter achieved removal efficiency larger than 60% at influent concentrations of 200 ppmv and lower, however, removal was significantly lower at 400 and 600 ppmv influent concentrations. Performance was improved by reseeding with cooking compost resulting in increased thermophilic bacterial population. Main byproduct formed was acetic acid with traces of formic acid. Mathematical modelling was used to successfully describe acetaldehyde concentration profiles.

1. Introduction

In 2015, the ethanol industry in the US hit a production milestone of 1 million barrel per day. Ethanol is the major biofuel produced and its production is expected to continue to increase (Fuels Association, 2016). However, hazardous air pollutants (HAPs) such as acetaldehyde, formaldehyde, and acrolein are emitted during production from Distilled Dry Grain Solubles (DDGS) dryers, fermentation tanks and distillation columns (Brady and Pratt, 2007). Federal regulations limit HAP emissions to 10 tons per year of any individual HAP and 25 tons per year for total HAPs for an ethanol plant to be classified as an 'Area Source' (US Environmental Protection Agency, 2009). Air pollution control equipment are essential to keep acetaldehyde, the major HAP of concern, in

* Corresponding author. United Arab Emirates University, United Arab Emirates.
E-mail address: alyhassan@uaeu.ac.ae (A.A. Hassan).

https://doi.org/10.1016/j.chemosphere.2019.124982
0045-6535/

compliance. The Environmental Protection Agency (EPA) has identified CO_2 scrubbing and regenerative thermal oxidation (RTO) as the best available control technologies (US Environmental Protection Agency, 2019). RTOs and scrubbers are usually used to control the dryers and fermentation, respectively. Both technologies are utility intensive and require large water and energy inputs. At an average ethanol plant producing annually 55 million gallons of denatured ethanol and 164,491 tons of DDGS, the RTO will be sized at about 18 MMBtu/hr. burning natural gas at about 155 MMSCF/yr.

An appealing alternative for the treatment of dilute HAPs is biofiltration (Delhoménie and Heitz, 2005). Traditional biofilters were evaluated for the removal of HAPs generated at an ethanol plant with limited success (Chen et al., 2010). Acetaldehyde and formaldehyde fumes were individually biodegraded in a 10 s empty bed resident time (EBRT). However, long-term treatment lead to pH decline and deteriorating performance. In another study, acetaldehyde was successfully degraded in a mixture of toluene and ethanol in a two-stage biofilter and 95% removal was maintained at 15 s EBRT (Jeong et al., 2006). Ethanol and acetaldehyde had removal yields over 97% at an elimination capacity (EC) of 14.67 $g\,m^{-3}\ hr^{-1}$ at influent concentration of 100 ppmv and 92–98% (EC 10.3 $g\,m^{-3}\ hr^{-1}$) at 70 ppmv, respectively (Jeong et al., 2006). A study on the biofiltration of a mixture of HAPs found that acetaldehyde had more biodegradation potential than ethanol (Fang, 2002).

A bio-trickling filter (BTF), where the pH could be controlled, was never evaluated for acetaldehyde emissions. The BTF is a packed-bed with bacteria growing on the media supplied intermittently by trickling nutrient liquid that could be buffered, contrary to the biofilter where acidification and media compaction is a problem (Delhoménie and Heitz, 2005; Crocker and Schnelle, 1998). In an ethanol plant, the onsite wastewater can be used as a trickling liquid since it includes all the required nutrients. The BTF has major advantages over scrubbers used to control the fermentation process such as reduction of water volume required for operation to about 5% and no additional chemical utilization (Gabriel and Deshusses, 2003). Moreover, significant cost savings may occur in comparison to an RTO controlling dryers, since no natural gas is required for operation.

DDGS dryers generate a hot air stream that is usually between 100 and 140 °C. After passing through a baghouse or cyclones for particulate control, the stream is cooled down to about 60 °C (Chen et al., 2010). Thermophilic bacterial growth is not usually encountered in a BTF. A comparison of thermophilic and mesophilic BTFs have shown that thermophilic treatment might be sometimes favorable; toluene was removed up to 90% at loading rates below 100 $g\,m^{-3}\ hr^{-1}$ (Wang et al., 2012), H_2S was removed up to 950 ppmv at 1.2 min residence time (Ryu et al., 2009), and methyl *tert*-butyl ether (MTBE) was removed up to 99% at 330 $g\,m^{-3}\ hr^{-1}$ (Moussavi et al., 2009). Sludge drying exhaust was treated with over 90% for Volatile Organic Compounds (VOCs), NH_3, and SO_2 (Yang et al., 2018).

Since acetaldehyde removal was never studied in a pH controlled BTF, the experimental plan was designed to evaluate the long-term performance of two independent BTFs removing acetaldehyde fumes operating at mesophilic and thermophilic conditions. BTF 'A' is operated at room temperature (21 °C) and BTF 'B' is operated at 60 °C to simulate emissions streams generated at ethanol plants. Several strategies were investigated to improve the performance including an increase of the liquid flowrate and utilization of different bacterial seeds. The study examines the removal efficiency under increasing loading rates with an emphasis on carbon balance closure and formation of byproducts.

2. Materials and methods

2.1. Experimental apparatus

Fig. 1 shows a full schematic of the experimental apparatus. The BTF media consisting of (0.3" - 0.5") pellets of diatomaceous earth (Celite 6 mm R-635; Lompoc, CA), was housed in a 3" internal diameter glass column. The media has a mean pore diameter of 20 μm, BET (Brunauer-Emmet-Teller) surface area of 0.27 m^2/g, and a bed density of 513 kg/m^3. It consists mainly of SiO_2 with a significant fraction of Al_2O_3. The beds were seeded with microorganisms by submerging overnight in return activated sludge obtained from the local wastewater treatment plant with additional glucose (2 $g\,L^{-1}$). The columns extend for 3′ above the top of the packing material, where the acetaldehyde laden air was introduced at the top to allow uniform mixing. Each BTF was equipped with sampling ports located at packed depths of 3, 13, 23, 33, and 36 inches. BTF 'B' was heated by a tape wrapped around the packed length of the column. A thermocouple placed through the fifth sampling port allowed for temperature control.

Following filtration of house air through a series of coalescing filters for the removal of bulk water, particles, and droplets, the air stream was split, and each channel was regulated to 8 L/min (for a corresponding EBRT of 30 s). Acetaldehyde (99.5% purity) obtained from Acros Organics (Pittsburgh, PA) was infused into the air stream through a septum. Applicable physical properties for acetaldehyde are presented in Table S1.

The nutrient solution, which was used for a once-through flow and was not recycled, consisted of essential inorganic salts and vitamins necessary to grow micro-organisms. Composition of the nutrient solution was similar to that reported elsewhere (Sorial et al., 1997). The nutrients were delivered intermittently by a misting nozzle. Sampled gas was directed towards either an Agilent Technologies 490 Micro Gas Chromatograph (μ-GC) with a thermal conductivity detector or an Agilent 490 GC/MS instrument (Santa Clara, CA).

2.2. Analytical methods

The GC/MS system was equipped with 30 m, 0.25 mm I.D. HP-5MS column. The GC was operated in 'Splitless mode' with an inlet temperature of 250 °C, an isothermal oven temperature of 30 °C, and a helium carrier gas flow rate of 1 mL/min. The injection valve was maintained at 80 °C and contained a 0.25 mL loop. A retention time of 1.46 min for acetaldehyde was obtained under these conditions. The detection limit was 0.5 ppmv. All acetaldehyde measurements were collected with six replicates.

The μ-GC was equipped with a two-channels; one channel used to measure O_2 and N_2 contained a 10 m MS5A heated injector maintained at 60 °C with a channel temperature of 75 °C and the other channel, used to measure CO_2, contained a 4 m PPQ module with an injector temperature of 50 °C and a column temperature of 55 °C.

Analysis of the liquid effluent included volatile suspended solids (VSS), chemical oxygen demand (COD), nitrate, and pH. VSS was determined using Methods 2540 D and 2540 E in Standard Methods (Water Environmental Federation and American Public Health Association, 2005), COD was determined using Hach (Loveland, Colorado) 820 vials. Nitrate concentration was determined using a Dionex IonPac™ (Pittsburgh, PA) AS22 ion chromatography instrument equipped with an analytical 4 × 250 mm column and a suppressed conductivity detector. The eluent used was 4.5 mM Na_2CO_3 and 1.4 mM $NaHCO_3$ with a flow rate of 1.2 mL/min. Temperature was 30 °C, applied current was 31 mA, injector

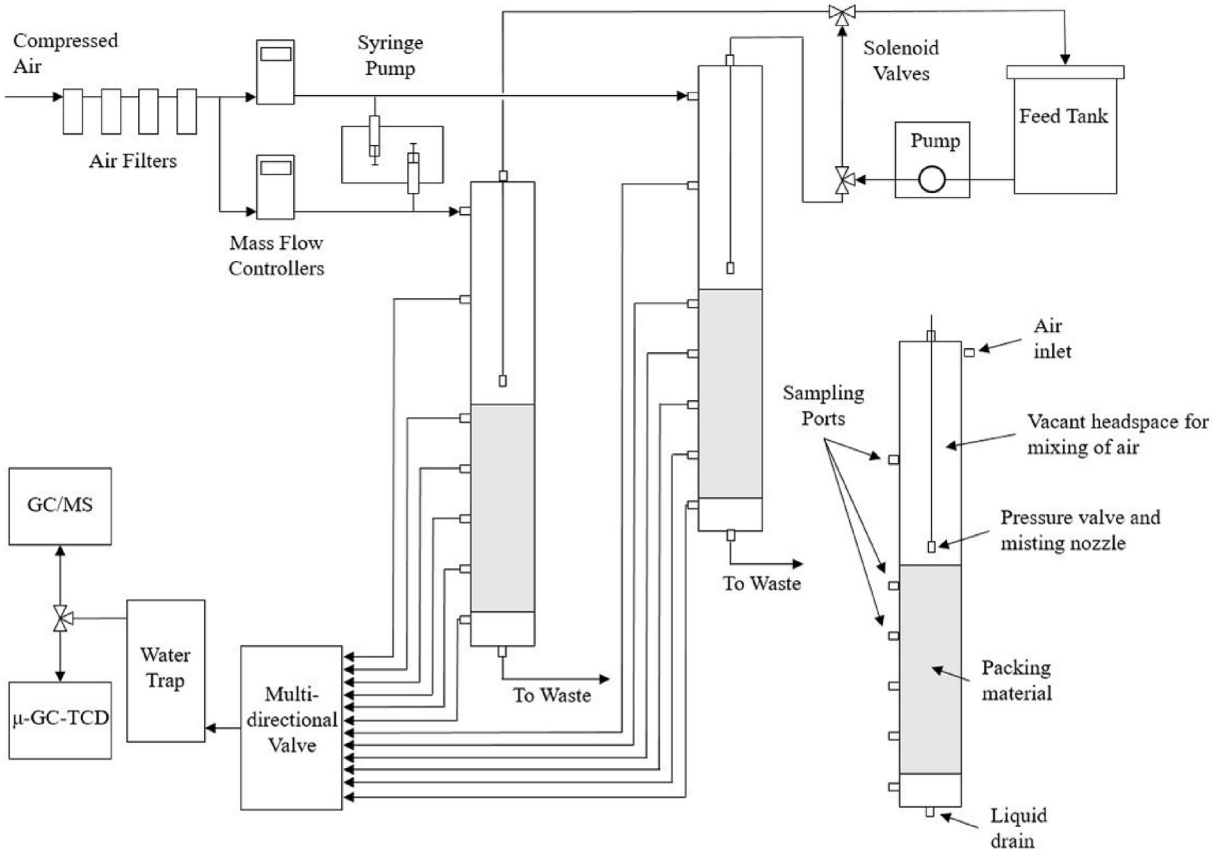

Fig. 1. Schematic of experimental apparatus.

volume was 10 μL and the storage solution was 100 mM $NaHCO_3$.

3. Results and discussion

Each BTF was operated at constant influent concentration, which was increased in a stepwise manner to form a total of six consecutive phases. A typical ethanol plant emission concentration of 20 ppmv was chosen as the starting concentration, and the highest concentration, 600 ppmv, represents more than one order of magnitude higher than expected plant emissions. The influent concentration, loading rate and corresponding average elimination capacity are shown in Table 1 for each BTF. The duration mentioned in the Table represents stable operation after a brief acclimation period. Acclimation periods were observed only during Phases I and II and were 5 and 3 days, respectively.

Starting from Phase III stagnation, a biomass control technique, was applied. During stagnation, gaseous and liquid inputs to the BTFs were halted. Variability in the measured influent concentration was observed in each BTF, starting at Phase IV. This is explained by the high vapor pressure of acetaldehyde which results in rapid volatilization affecting high syringe pump flow rates. While target influent concentrations are presented in Table 1, actual measured concentrations in ppmv at phases IV, V, and VI, were 170 ± 49.3, 361 ± 117, and 417 ± 77 for BTF 'A' and 168 ± 66.2, 330 ± 128, and 352 ± 112 for BTF 'B', respectively. There was no significant difference between A and B although they were independently fed. It should be noted that the daily reported concentration is the average of 5 consecutive injections. The observed differences among these injections were significantly less than that observed day to day. Complete uptake of nitrates in BTF 'A' prompted an extension to Phase V. The nitrate concentration of the influent solution was increased from 495 mg L^{-1} to 741 mg L^{-1} for an additional two weeks. This is conducted to ensure that the removal of acetaldehyde would not be limited by nitrate availability. This same

Table 1
Different phase of operation including duration, influent concentration, loading rate, elimination capacity, and removal efficiency for both BTFs ('A' – 21 °C and 'B' – 60 °C). Error ranges represent one standard deviation.

Phase	Duration (days)	Influent Concentration (ppmv)	Target Loading Rate (g m^{-3} hr^{-1})	Average Elimination Capacity (g m^{-3} hr^{-1})		Average Removal Efficiency (%)	
				BTF 'A'	BTF 'B'	BTF 'A'	BTF 'B'
I	18	20	4.2	4.2 ± 1.00	4.2 ± 1.20	100 ± 0.0	96.2 ± 10.4
II	21	40	8.4	8.4 ± 2.84	8.4 ± 3.00	100 ± 0.0	84.9 ± 17.8
III	18	100	22.6	20.0 ± 5.2	15.1 ± 5.2	100 ± 0.0	58.4 ± 16.8
IV	28	200	45.3	38.4 ± 11.2	20.3 ± 17.6	99.8 ± 0.3	60.8 ± 29.5
V	42	400	90.6	74.4 ± 26.0	17.6 ± 24.8	90.8 ± 13.8	19.4 ± 23.2
VI	23	600	136.0	82.86 ± 15.2	2.68 ± 16.4	83.2 ± 12.5	9.3 ± 15.2

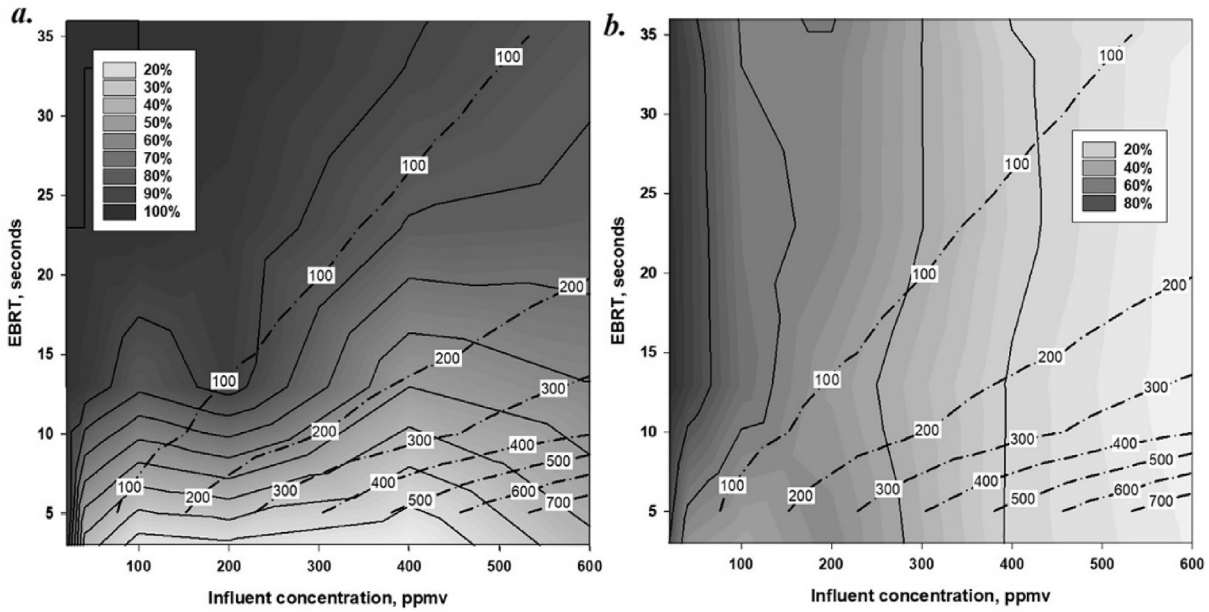

Fig. 2. Removal efficiency as a function of EBRT and influent concentration (a) for BTF 'A' (21 °C) and (b) for BTF 'B' (60 °C). The dash-dot lines represent the loading rate in g m^{-3} hr^{-1}.

amount of additional nitrate was supplied through phase VI.

Fig. 2 shows the removal efficiency of each BTF as a function of EBRT and influent concentration. Removal, over 90%, was achieved consistently for EBRTs larger than 11 s at influent concentrations of approximately 50 ppmv and below for both BTFs. At BTF 'A', achieving 90% removal efficiency at 600 ppmv required just over 30 s. At loading rate of 200 g m^{-3} hr^{-1}, 60% removal efficiency could be maintained at 7 s EBRT. However, the EBRT didn't influence the removal efficiency at BTF 'B', suggesting that the top portion of the bed was responsible for most of the acetaldehyde degradation.

Fig. 3 shows the loading rate versus the elimination capacity for both BTFs. For BTF 'A', the elimination capacity increased proportionally to the loading rate up to 36 g m^{-3} hr^{-1}. High elimination capacity was still observed at higher loading rates. A maximum elimination capacity could not be established. The highest reported EC of 82.86 g m^{-3} hr^{-1} is three times greater than that reported by other authors who studied acetaldehyde (Chen et al., 2010). The superior performance is explained by the buffering capacity of the trickling liquid that enabled the bed to be subjected for elevated loading rates that couldn't be achieved before without acidification.

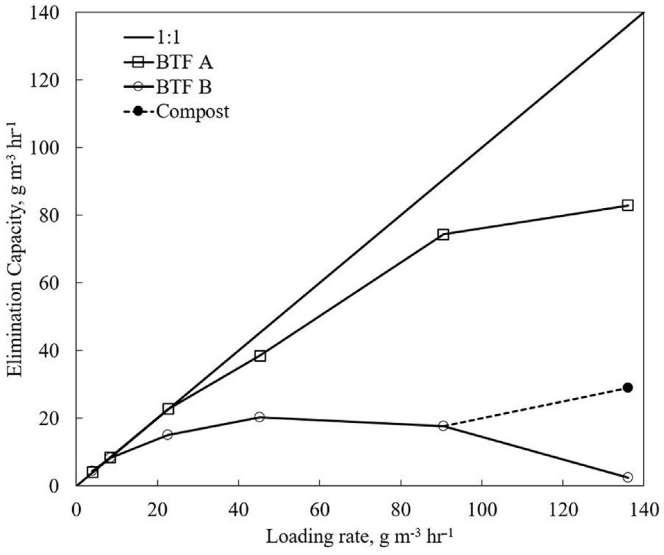

Fig. 3. Elimination capacity versus loading rate curves for each BTF. The solid data point connected to the curve for BTF 'B' refers to results obtained after re-seeding BTF 'B' with a slurry prepared from cooking compost.

BTF 'B' performed more poorly than BTF 'A' at higher concentrations. The maximum elimination capacity was obtained at a loading rate of 36 g m^{-3} hr^{-1} at a value of 28.9 g m^{-3} hr^{-1}. Additionally, the elimination capacity for BTF 'B' is seen to decline suggesting biomass loss. The point labelled 'compost' refers to results described in section 3.3, in which BTF B was reseeded with microorganisms from a compost slurry in attempts to improve its performance. Acetaldehyde has never been studied in a thermophilic BTF; however other compounds have been degraded at temperatures ranging from 50 to 60 °C with a high removal rate. MTBE was degraded with a maximum reported EC of 640 g m^{-3} hr^{-1}. (Moussavi et al., 2009). Isobutyraldehyde and 2-pentanone were individually degraded with ECs of 139 and 63 g m^{-3} hr^{-1}, respectively (Luvsanjamba et al., 2007). Toluene was successfully degraded in a GAC packed BTF with an EC of 150 g m^{-3} hr^{-1} (Wang et al., 2012). Finally, ethanol and trimethylamine were each individually degraded with ECs of 140 g m^{-3} hr^{-1} (Cox et al., 2001; Wei et al., 2015). In comparison, the EC reached by BTF 'B' is modest and higher removal may have been possible using a gentler heating apparatus. More on this will be discussed in Section 3.2.

3.1. Performance of BTF 'A'

Fig. 4 shows the target influent concentrations, effluent concentrations, and removal efficiency of acetaldehyde throughout the entire study. As seen in the figure, complete removal of acetaldehyde was achieved through phase IV. In phase V, approximately 90% removal was achieved. The removal efficiency was changing erratically in phase VI due to variability in the loading conditions however the removal dropped below 50% only once and below 60% on only three days.

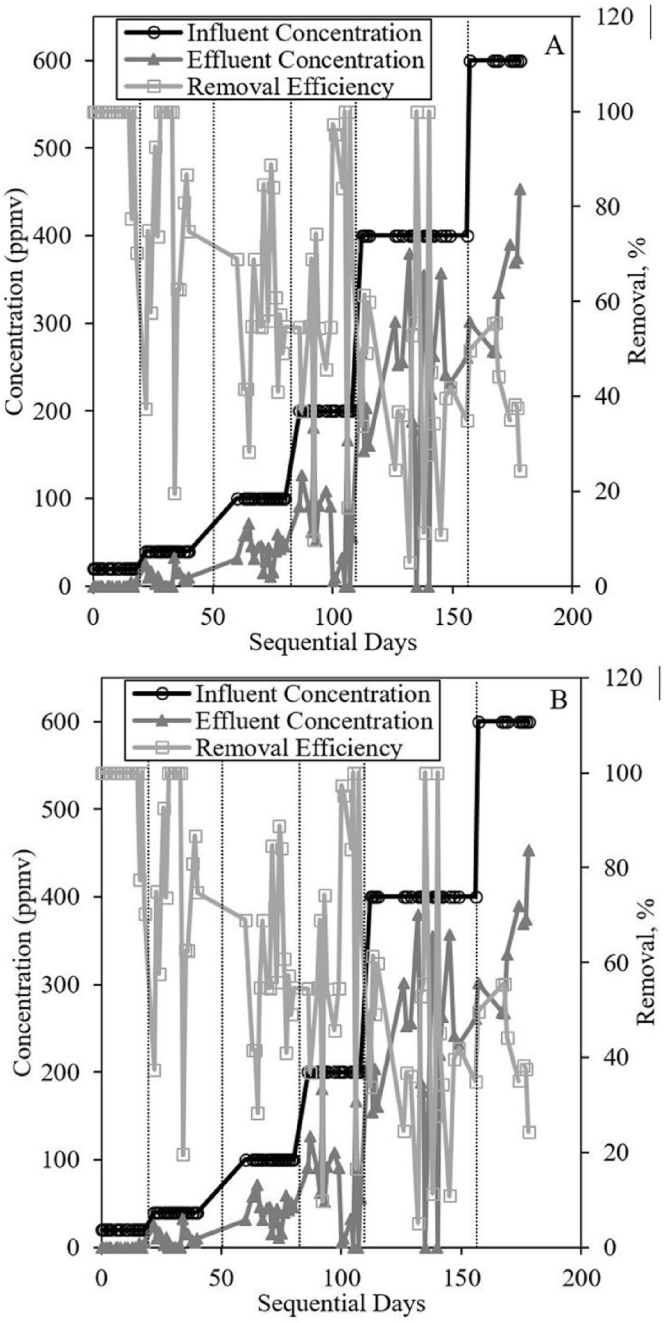

Fig. 4. Influent concentration, effluent concentration and removal efficiency for the duration of the study. Plot (a) is for BTF 'A' at 20 °C and plot (b) is for BTF 'B' at 60 °C. Vertical dotted lines indicate a transition between concentration phases.

The measured pH of the nutrient solution in the holding tank was on average 8.53 ± 0.44. The average change in pH between the influent and effluent was 0.83 ± 0.27, 0.36 ± 0.31 and 0.26 ± 0.37 for Phases IV, V, and VI, respectively. It is expected that the pH will increase due to aerobic degradation of acetaldehyde. At higher concentration other acidic byproducts were formed. Their concentration was increased with elevated influent acetaldehyde concentration decreasing the pH of the effluent liquid. Regardless, at no point did the bed acidify as observed in a previous study (Chen et al., 2010).

VSS of the liquid effluent increased with increasing loading rates for BTF 'A', however VSS spiked considerably in phase VI. The maximum VSS measured in Phases III, IV, and V were 21.0, 24.7, and 27.3 mg L^{-1} respectively while in Phase VI the maximum VSS was 86.4 mg L^{-1}. The increase in VSS during phase VI suggests biomass growth greater than the media holding capacity. Effluent COD in mg L^{-1} averaged 77.9 ± 33.2, 915.8 ± 87.0 and 1960 ± 1387 during Phases IV, V, and VI, respectively. This is again attributable to loss of biomass but also to increased byproduct concentrations. The composition of the effluent COD will be discussed in detail in Section 3.5.

3.2. Performance of BTF 'B'

The heated BTF achieved 96% removal in Phase I, however through the later phases, removal steadily declined reaching 85%, 58%, 61% in phases II, III, and IV, respectively. In phases V and VI, the removal decreased significantly reaching only 19% and 9.3%, respectively. The most probable explanation for this poor performance is the lack of nutrient liquid and sufficient thermophilic organisms in BTF 'B', as discussed in Section 3.3. Exposure to these conditions over time led to biofilm deterioration. Visual inspection strongly indicated that BTF 'B' contained significantly less biomass than BTF 'A'. Furthermore, while the biomass in BTF 'A' was observed to both grow thicker and to move downward through the media as the concentration of acetaldehyde was increased, no such changes were noticeable in BTF 'B'.

The poor performance is attributed to other factors as well. First, the solubility of acetaldehyde decreases by approximately a factor of ten as temperature increases from 20 °C to 60 °C resulting in low availability of acetaldehyde for biodegradation in the liquid phase. At an air flowrate of 8 L/min and a saturated water vapor pressure of 19.92 kPa at 60 °C, the amount of vaporized water is equal to 1.5 L/day of liquid equivalent. This is a comparable amount to the volume of water fed and suggests that BTF 'B' may have had little liquid water available. Temperature control was performed using a thermocouple placed in the fifth sampling port. This thermocouple measured the temperature just at the edge and did not extend into the interior of the media. The temperature of the column was measured manually using an infrared thermometer gun and the temperature set point was adjusted until the apparent temperature reading was 60 °C. Furthermore, the thermostat exhibited significant lag time and occasional overshoot. During overshoot, the infrared thermometer would read temperatures up to 100 °C. These periods of extreme temperature prevented biofilm from forming.

Other phenomena were also observed as a result of the heating of BTF 'B'. Due to evaporation of the nutrient solution supplied to BTF 'B', accumulation of salts was observed. This accumulation resulted in periodic 'flushing events' whereby during a dip in temperature, deposited salts would be flushed in the effluent liquid by a sudden increase in liquid flow rate. The effluent during these events appeared dark in color due to concentrated ferric ion. The effluent from one of these events registered a total fixed solids concentration of 6200 mg L^{-1}. The pH of the effluent during one of these events was 10.2, an increase of 2.6 log units from the influent solution on that day.

The average change in pH between the effluent and the influent solution was 0.11 ± 0.77, −0.64 ± 1.23, and 0.66 ± 1.69 during Phases IV, V, and VI, respectively. These results show that within the same phase, pH changed erratically. This behavior could be explained by the frequent observed flushes. VSS for BTF 'B' increased on average from 34.1 mg L^{-1} in Phase III to 39.5 mg L^{-1} in Phase IV. In Phases V and VI, the VSS decreased to 21.3 and 12.8 mg L^{-1} respectively. Although VSS decreased as loading rate increased, COD exhibited the opposite trend. Average COD for Phases III through VI were 171, 144, 242, and 375 mg L^{-1} respectively. As with BTF 'A', this trend suggests an increase in soluble

byproducts. At lower concentrations, BTF 'B' generated larger concentrations of COD than BTF 'A' suggesting that increased temperature results in incomplete degradation of acetaldehyde. In Phases V and VI, there was not enough biomass to support a high removal rate in BTF 'B' resulting in lower COD concentrations than in BTFBTF 'A'.

3.3. Improving the performance of BTF 'B'

Several attempts were made to remedy the deficiency in removal of BTF 'B' at 600 ppmv influent. Since the BTF was losing influent nutrient liquid in the form of vapor, the liquid flowrate was increased from 1.2 to 2.7 L/day. After estimating the amount lost due to evaporation to be 1.5 L/day, the remaining 1.2 L/day is comparable to that rate used for BTF 'A'. Collected effluent volume increased from 0.87 ± 0.34 to 2.7 ± 0.22 L/day. The increase in water volume did not result in the expected increase in removal efficiency.

Since BTF 'B' had lost most of its biomass, a new inoculant was needed. Initially, the column was seeded with anaerobic sludge kept at 35 °C. The availability of additional thermophilic bacteria consortium could enhance the performance by providing a greater variety of micro-organisms which will survive at elevated temperature. Therefore, compost from a cooking pile at 120 °F was used to reseed the column. The compost was suspended in water and acetaldehyde fumes were bubbled through the slurry for one week while heated to a temperature of 40 °C. Finally, the slurry was strained and used to submerge the media for 6 h. After an additional two weeks of operation, an average elimination capacity of 29 g m^{-3} h^{-1} was observed with an average removal efficiency of 21.3%. This result is noted in Fig. 3 and marks a reasonable improvement from the previously recorded elimination capacity for phase VI. Furthermore, it appears to progress logically from the data points corresponding to phases I–IV and may reflect a return to biofilter operation which is not limited by biodegradation.

3.4. Identification of byproducts

In the event of incomplete acetaldehyde degradation, byproducts may be expelled from the bed with the liquid effluent or in the gas. Expected degradation byproducts in the liquid are acetate, formate, ethanol, methanol and formaldehyde. To identify byproducts, ion chromatography was used to analyze liquid effluent samples beginning in phase V. Acetate was identified as a major byproduct; however, it was still a fraction of the total COD. Formate was also identified, however no formate was detected in BTF 'A' and only trace amounts were detected in BTF 'B'. For BTF 'A', 140 mg L^{-1} of acetate was detected during phase V and up to 625 mg L^{-1} was detected during phase VI. For BTF 'B', up to 227 mg L^{-1} of acetate were detected during phase V and up to 401 mg L^{-1} were detected during phase VI. A maximum of 0.8 mg L^{-1} of formate was detected throughout all phases.

Liquid samples were also collected from each sampling port of BTF 'A' during phase VI to identify depth-wise trends in byproduct formation, however neither acetate nor formate were detected in these samples. Liquid samples could not be collected from BTF 'B', even during the period of increased water supply. The creation of ethanol, methanol, and formaldehyde as volatile byproducts was investigated using a DB wax column in the GC/MS, nevertheless, none were detected. This suggests that the main degradation pathway goes through the aldehyde dehydrogenase enzyme, which transforms acetaldehyde to acetic acid through converting NAD^+ to NADH (nicotinamide adenine dinucleotide). The required oxygen molecule is obtained by oxygen.

3.5. Carbon mass balance

Fig. 5 shows the organic carbon mass balance for each BTF. The only source of input carbon is influent gaseous acetaldehyde. Inorganic carbon, such as the carbonate in the nutrient solution is not considered. Background CO_2 found in the house air is considered but is subtracted from effluent CO_2 and so is not depicted in the figure. Sources of effluent carbon in the gas phase include undegraded acetaldehyde and CO_2 produced by metabolic processes. COD is the only source of effluent carbon in the liquid phase. COD composition includes VSS, soluble byproducts, and dissolved

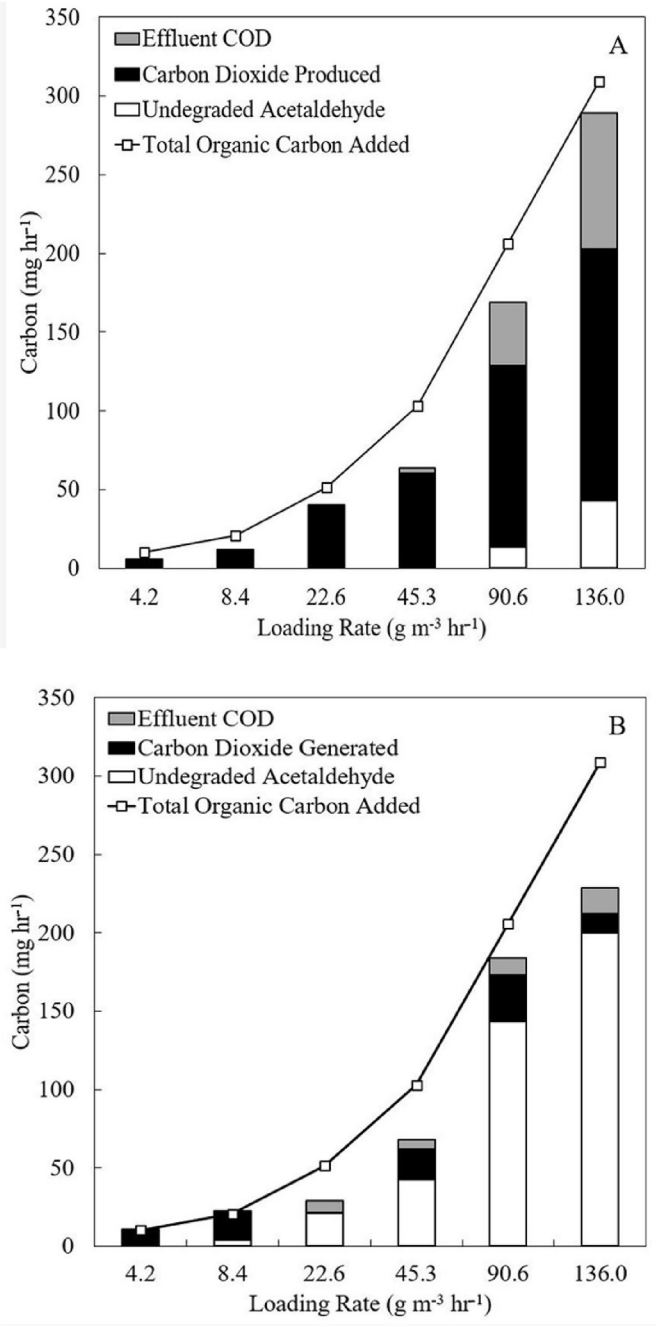

Fig. 5. Carbon mass balance for (a) 20 °C (BTF 'A') and (b) 60 °C (BTF 'B'). The line plot shows the amount of influent carbon to each BTF and the stacked bar graph shows the composition of carbon in effluent sources.

acetaldehyde. To convert the COD of the effluent liquid to a mass of carbon all components of the total COD were assumed to have the chemical identity of acetate, since this was the major byproduct identified. For BTF 'A', acetate composed 20% of effluent COD for phase V and 42% for phase VI. The effluent COD contribution from dissolved acetaldehyde is not expected to be significant because the liquid collection containers are open to the atmosphere allowing this acetaldehyde to volatilize. The remaining COD contribution is expected to result from microorganisms. Effluent water in the unheated BTF was visibly cloudy throughout the highest two concentration phases, suggesting that some loss of biomass was indeed occurring. The relative amounts of influent carbon transformed to CO_2 and to biomass are also of interest. For BTF 'A', between 48% and 59% of influent carbon was transformed to CO_2 except for Phase III, during which 89% of carbon was transformed. For BTF 'B', acetate accounted for almost all the effluent COD in both phases V and VI. The mass balance shows that undegraded acetaldehyde accounted for the majority of effluent carbon and that CO_2 production and COD generation did not increase with loading rate. The consistent CO_2 and COD values over the operating period suggest that a maximum elimination capacity was reached, and that increased loading rate does not result in increased biodegradation.

3.6. Modelling

Two mathematical models were developed to describe the variations in acetaldehyde concentration throughout the bed depth. Model 1 operates on the assumption that as acetaldehyde is degraded in the liquid, it is instantaneously repartitioned to achieve vapor liquid equilibrium (VLE). The assumptions relevant to its development are shown below.

1. The system attains instantaneous VLE.
2. No radial variation in parameters is expected.
3. Flow of water through the bed is continuous and uniform.
4. Degradation reactions occur by a first order rate law.
5. The ideal gas law applies to all gaseous species.
6. Variation in biofilm density does not affect the void ratio or rate constant.

Consider that VLE for a highly volatile species is described by Henry's law

$$C = Hy \tag{1}$$

where C is the liquid phase concentration, H is the Henry's law constant, and y is the gas phase mole fraction. All modelling parameters, with units, are defined in Table S2.

The total moles of a volatile species at an arbitrary location in the BTF is the sum of the moles in the liquid and gaseous phases. Substitution of Henry's law into this mole balance yields an expression relating the gas phase mole fraction of acetaldehyde to the total moles of acetaldehyde in both phases.

$$y = \frac{n}{\frac{Q_G}{\overline{V}_{ig}} + Q_L H} \tag{2}$$

Here, n is the total molar flow rate of acetaldehyde, Q_G is the volumetric gas flow rate, Q_L is the volumetric liquid flow rate and V_{ig} is the specific volume of an ideal gas. A mole balance over a differential volume of BTF in the liquid phase shows that the total moles of acetaldehyde varies according to

$$dn = -Q_L k H y \frac{dz}{v_L} \tag{3}$$

where k is a first order degradation rate constant, n is the total moles of acetaldehyde, and z is the spatial coordinate corresponding to bed depth. Combining Eq. (2) with Eq. (3) and integrating results in

$$n = n_0 e^{-\alpha z} \tag{4}$$

where alpha is a lumped parameter equal to

$$\alpha = \frac{Q_L k H \overline{V}_{ig}}{v_L \left(Q_G + Q_L H \overline{V}_{ig}\right)}. \tag{5}$$

One additional substitution of Eq. (2) provides an expression for the variation of gas phase mole fraction with depth.

$$y = y_0 e^{-\alpha z} \tag{6}$$

Concentration profiles of acetaldehyde were collected at all phases and are shown in supplemental materials. The profiles were used to generate apparent exponential decay in accordance with Eqs. (5) and (6) fitting for 'k' using least square methods. The values obtained for each phase are shown in Table 2. Note in this table that the quantities K_La and K_Ga are lumped parameters fitted using Model 2, to be developed shortly. Using the best fit values of the rate constants, equation (6) was plotted alongside the measured acetaldehyde concentration profiles. These plots are shown in Fig. 6. Note that the line representing Model 2 coincides on top of the line representing Model 1, making it difficult to recognize it.

Note the first order rate constant is inversely proportional to acetaldehyde concentration. This relationship is expected considering a Monod kinetic model. Plotting the inverse of the first order rate constant versus acetaldehyde concentration yields a coefficient of determination equal to 0.94, suggesting that the observed variability is due to deviation of the assumed kinetics from the Monod model. The half maximal velocity constant and maximum rate of substrate utilization derived from this analysis are 16.6 mg L^{-1} and 633 mg L^{-1} hr^{-1}, respectively.

Model 1 makes use of the assumption that biodegradation is kinetically limited. To evaluate the validity of this assumption, Model 2 that does not assume instantaneous equilibrium and instead considers the rate of mass transfer between gas and liquid phases was developed. Two resistance film theory was used to describe the mass transfer to develop Model 2. The governing equations for Model 2 can be found by considering a mass balance written around a differential volume of bed volume with cross sectional area 'A' and height 'dz'. In simplified form, these equations are:

$$\frac{dC}{dz} = \left(\frac{K_L a A H}{Q_L}\right) y - \frac{A}{Q_L}(K_L a + k) C \tag{7}$$

Table 2
Best fit rate constants and overall mass transfer coefficients for BTF 'A'.

Phase	Concentration (ppmv)	k (s^{-1})	K_La (s^{-1})	K_Ga (s^{-1})
I	20	0.01058	0.478	62.6
II	40	0.00152	0.321	41.6
III	100	0.00101	0.367	47.3
IV	200	0.00124	0.230	29.8
V	400	0.00055	0.424	54.7
VI	600	0.00037	0.343	44.5

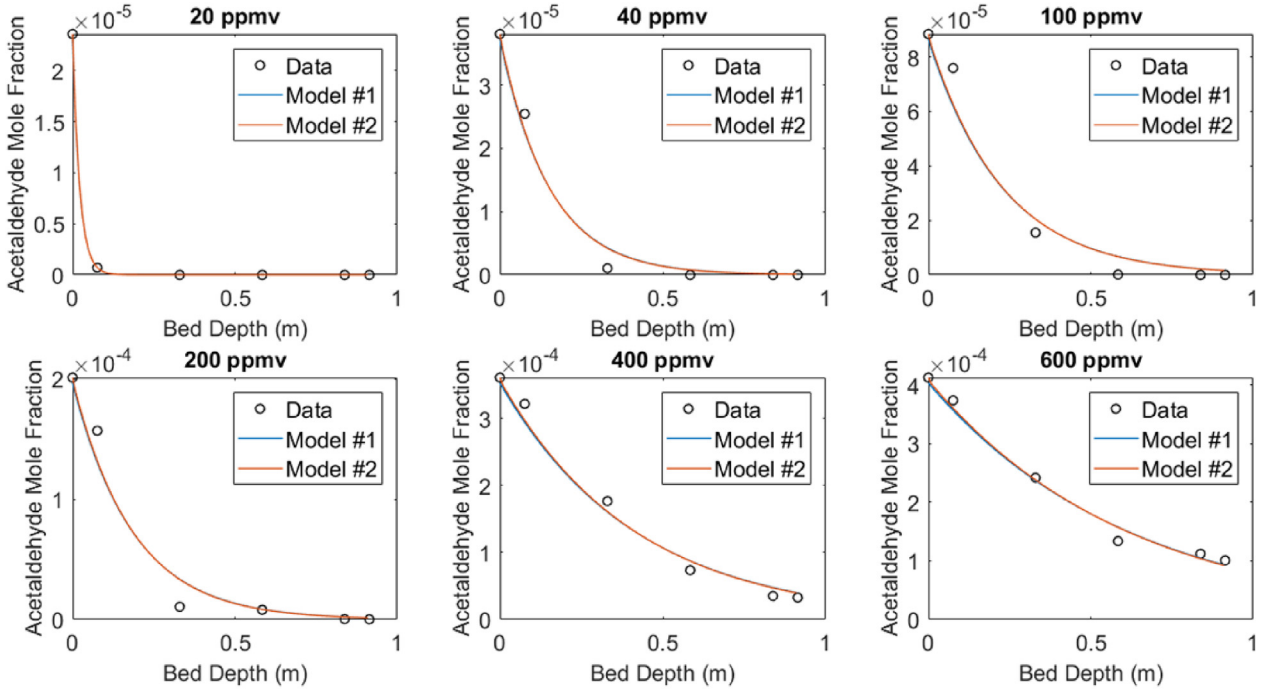

Fig. 6. Comparison of the fitted curves for Models 1 and 2 to measured gas phase acetaldehyde concentration profiles.

$$\frac{dy}{dz} = -\left(\frac{K_G aA}{Q_G}\right)y + \left(\frac{K_G aA}{Q_G H}\right)C \tag{8}$$

with initial conditions given by:

$C(0) = 0$
$y(0) = y0$

In equations (7) and (8), a is the specific interfacial area, and K_L and K_G are overall mass transfer coefficients as defined in two film resistance theory. The analytical solution to these equations is:

$$y(z) = \frac{y_0}{2C_2}\left((C_2 + C_4 + C_5 - C_6)e^{\frac{A(C_2-C_1)}{C_3}z} + (C_2 - C_4 - C_5 + C_6)e^{-\frac{A(C_1+C_2)}{C_3}z}\right) \tag{9}$$

$$C(z) = \frac{y_0 HC_5}{C_2}\left(e^{\frac{A(C_2-C_1)}{C_3}z} - e^{-\frac{A(C_1+C_2)}{C_3}z}\right) \tag{10}$$

In equations (9) and (10), the constants C_1 through C_6 are lumped parameters used for convenience. They are defined as:

$$C_1 = HkQ_G + HK_L aQ_G + HK_G aQ_L \quad C_3 = 2HQ_G Q_L \quad C_5 = HK_L aQ_G$$

$$C_2 = \sqrt{C_1^2 - 4H^2 kK_G aQ_G Q_L} \quad C_4 = HkQ_G \quad C_6 = HK_G aQ_L$$

In this model, K_L, K_G, a and k are unknown. Since K_L and K_G always appear multiplied with an a and since the individual value of these parameters is of little practical importance, they are often lumped together as the quantities $K_L a$ and $K_G a$. Using the value of 'k' obtained from the analysis of Model 1, the value of these lumped parameters was determined by a two-dimensional least squares regression. Considering that the value of $K_G a$ is two orders of magnitude larger than the that of $K_L a$, it can be concluded that the mass transfer rate is controlled by the resistance in the liquid film.

For all phases, the concentration profile curves generated by the two models are indistinguishable. A possible interpretation of this detail is that the 'fast to equilibrium' assumption used by Model 1 is valid. If this assumption was not valid then the results obtained using Model 2, in which this assumption was abandoned, should be noticeably dissimilar. The validity of the 'fast to equilibrium' assumption implies that acetaldehyde degradation is kinetic limited – not transport limited.

4. Conclusions

Utilization of BTFs as the main air emission control device in place of scrubbers and RTOs is feasible for both fermentation tank and DDGS dryers' emission streams. Both the 21 °C and 60 °C BTF successfully degraded acetaldehyde fumes with high removal efficiency at concentrations expected from ethanol plant emissions. At elevated temperatures, seeding with cultivated thermophilic bacteria will be necessary for long term effectiveness and care must be taken to ensure adequate water supply. The 20 °C BTF has shown that it could accommodate spikes in concentrations at least one order of magnitude larger than the typical expected concentration.

Acknowledgements

This work was supported by the Nebraska Water Center through USGS grant104b (Year 2017); the Nebraska Center for Energy Sciences Research (NCESR), Cycle 13.

Appendix A. Supplementary data

Supplementary data to this article can be found online at

https://doi.org/10.1016/j.chemosphere.2019.124982.

Declaration of interest statement

None.

References

Brady, D., Pratt, G.C., 2007. Volatile organic compound emissions from dry mill fuel ethanol production. J. Air Waste Manag. Assoc. 57, 1091–1102.

Chen, L.J., Bangs, K.M., Kinney, K.A., Katz, L.E., Seibert, A.F., 2010. Biofiltration of simulated air pollutants from distillers dried grains with solubles (DDGS) dryer vents at corn-derived ethanol production facilities. Environ. Prog. Sustain. Energy 29, 116–126.

Cox, H.H., Sexton, T., Shareefdeen, Z.M., Deshusses, M.A., 2001. Thermophilic biotrickling filtration of ethanol vapors. Environ. Sci. Technol. 35, 2612–2619.

Crocker, B., Schnelle, K., 1998. Air pollution control for stationary sources. Encycl. Environ. Anal. Remediat. 1, 150–169.

Delhoménie, M.-C., Heitz, M., 2005. Biofiltration of air: a review. Crit. Rev. Biotechnol. 25, 53–72.

Fang, Y., 2002. New developments of biotrickling filters: experiments and theories. In: Chemical Engineering. University of Cincinnati, OhioLink.

Fuels Association, Renewable, 2016. Fueling a High Octane Future: 2016 Ethanol Industry Outlook.

Gabriel, D., Deshusses, M.A., 2003. Retrofitting existing chemical scrubbers to biotrickling filters for H2S emission control. Proc. Natl. Acad. Sci. 100, 6308–6312.

Jeong, G.-T., Park, D.-H., Lee, G.-Y., Cha, J.-M., 2006. Application of two-stage biofilter system for the removal of odorous compounds. In: Twenty-Seventh Symposium on Biotechnology for Fuels and Chemicals. Springer, pp. 1077–1088.

Luvsanjamba, M., Sercu, B., Kertész, S., Van Langenhove, H., 2007. Thermophilic biotrickling filtration of a mixture of isobutyraldehyde and 2-pentanone. J. Chem. Technol. Biotechnol. : Int. Res. Process Environ. Clean Technol. 82, 74–80.

Moussavi, G., Bahadori, M.B., Farzadkia, M., Yazdanbakhsh, A., Mohseni, M., 2009. Performance evaluation of a thermophilic biofilter for the removal of MTBE from waste air stream: effects of inlet concentration and EBRT. Biochem. Eng. J. 45, 152–156.

Ryu, H.-W., Yoo, S.-K., Choi, J.M., Cho, K.-S., Cha, D.K., 2009. Thermophilic biofiltration of H2S and isolation of a thermophilic and heterotrophic H2S-degrading bacterium, Bacillus sp. TSO3. J. Hazard Mater. 168, 501–506.

US Environmental Protection Agency, 2009. 42 U.S. Code §7412, in: Section 112(a), pp. 5840-5868. https://www.govinfo.gov/content/pkg/USCODE-2009-title42/pdf/USCODE-2009-title42-chap85-subchapI-partA-sec7412.pdf.

US Environmental Protection Agency, 2019. RACT/BACT/LAER clearinghouse. In: Clean Air Technology Center. https://www.epa.gov/catc/ractbactlaer_clearinghouse_rblc_basic_information.

Wang, C., Kong, X., Zhang, X.-Y., 2012. Mesophilic and thermophilic biofiltration of gaseous toluene in a long-term operation: performance evaluation, biomass accumulation, mass balance analysis and isolation identification. J. Hazard Mater. 229, 94–99.

Water Environmental Federation, American Public Health Association, 2005. Standard Methods for the Examination of Water and Wastewater. Washington, DC, USA.

Wei, Z., Huang, Q., Ye, Q., Chen, Z., Li, B., Wang, J., 2015. Thermophilic biotrickling filtration of gas–phase trimethylamine. Atmos. Pollut. Res. 6, 428–433.

Yang, K., Li, L., Ding, W., Liu, J., Xue, S., 2018. A full-scale thermophilic biofilter in the treatment of sludge drying exhaust: performance, microbial characteristics and bioaerosol emission. J. Chem. Technol. Biotechnol. 93, 2216–2225.